The Barley MLO Modulator of Defense and Cell Death Is Responsive to Biotic and Abiotic Stress Stimuli[1]

Pietro Piffanelli, Fasong Zhou, Catarina Casais, James Orme, Birgit Jarosch, Ulrich Schaffrath, Nicholas C. Collins, Ralph Panstruga, and Paul Schulze-Lefert*

The Sainsbury Laboratory, John Innes Centre, NR4 7UH Norwich, United Kingdom (P.P., F.Z., C.C., J.O., N.C.C.); Rheinisch-Westfälische Technische Hochschule Aachen, Institut für Biologie III, D–52074 Aachen, Germany (B.J., U.S.); and Max-Planck-Institut für Züchtungsforschung, Department of Plant Microbe Interactions, D–50829 Köln, Germany (R.P., P.S.-L.)

Lack of the barley (*Hordeum vulgare*) seven-transmembrane domain MLO protein confers resistance against the fungal pathogen *Blumeria graminis* f. sp. *hordei* (*Bgh*). To broaden the basis for MLO structure/function studies, we sequenced additional *mlo* resistance alleles, two of which confer only partial resistance. Wild-type MLO dampens the cell wall-restricted hydrogen peroxide burst at points of attempted fungal penetration of the epidermal cell wall, and in subtending mesophyll cells, it suppresses a second oxidative burst and cell death. Although the *Bgh*-induced cell death in *mlo* plants is spatially and temporally separated from resistance, we show that the two processes are linked. Uninoculated mutant *mlo* plants exhibit spontaneous mesophyll cell death that appears to be part of accelerated leaf senescence. *Mlo* transcript abundance increases in response to *Bgh*, rice (*Oryza sativa*) blast, wounding, paraquat treatment, a wheat powdery mildew-derived carbohydrate elicitor, and during leaf senescence. This suggests a broad involvement of *Mlo* in cell death protection and in responses to biotic and abiotic stresses.

Homozygous mutant (*mlo*) alleles of the *Mlo* gene confer broad spectrum disease resistance to the biotrophic powdery mildew fungus, *Blumeria graminis* f. sp. *hordei* (*Bgh*; Jørgensen, 1992). The resistance is manifested in the failure of the fungus to penetrate the epidermal cell wall, and at these sites, cell wall remodeling and oxidative cross-linking processes fortify the cell wall (Thordal-Christensen et al., 1997; von Röpenack et al., 1998; Hückelhoven et al., 1999). Although cell wall reinforcement is likely to contribute to the resistant phenotype, other yet unknown molecular events may lead to abortion of fungal attack. Although the wild-type *Mlo* gene in effect acts as a negative regulator of a defense response, wild-type *Ror1* and *Ror2* are two genes that are required for full expression of *mlo* resistance to *Bgh*, but not race-specific resistance (Freialdenhoven et al., 1996; Peterhänsel et al., 1997). It is curious that powdery mildew-resistant *mlo* plants exhibit enhanced susceptibility to the fungal pathogens *Magnaporthe grisea* and *Bipolaris sorokiniana* (Jarosch et al., 1999; Kumar et al., 2001).

Mutant *mlo* plants exhibit a spontaneous mesophyll cell death phenotype that is compromised by *ror1* and *ror2* mutations (Wolter et al., 1993; Peterhänsel et al., 1997). In this respect, *mlo* mutations resemble other mutations known to enhance host cell death processes along with disease resistance (Shirasu and Schulze-Lefert, 2000). Many of these mutants constitutively express pathogen-related (*PR*) genes, but in barley (*Hordeum vulgare*) *mlo*, maize (*Zea mays*) *lls1*, and Arabidopsis *lsd1* and *edr1* plants, pathogen inoculation is required to trigger an enhanced defense response (Jabs et al., 1996; Frye and Innes, 1998; Simmons et al., 1998). These four genes have been isolated (Büschges et al., 1997; Dietrich et al., 1997; Gray et al., 1997; Frye et al., 2001), and encode dissimilar proteins.

Barley MLO is the prototype of a family of seven-transmembrane (7-TM) proteins that is found in higher plants and bryophytes, but not in prokaryotes, yeast, or animals (Büschges et al., 1997; Devoto et al., 1999). In Arabidopsis, the family comprises 15 members that share a common membrane-spanning topology (A. Devoto, H.A. Hartmann, P. Schulze-Lefert, and R. Panstruga, unpublished data). Sequence diversity between MLO family members within a species, their 7-TM domain topology, and their location in the plasma membrane are reminiscent of fungal and animal G-protein-coupled receptors (Bockaert and Pin, 1999; Devoto et al., 1999). However, recent data indicate that MLO-mediated defense suppression in barley functions independently of heterotrimeric G-proteins and that calmodulin interacts with MLO to dampen defense reactions against the powdery mildew fungus (Kim et al., 2002). In addition, a small GTP-binding protein of the barley RAC family (RACB) may play a role in MLO-mediated powdery

[1] This work was supported by the Gatsby Charitable Organization and the Max-Planck Society (grants to P.S.-L.), by the Biotechnology and Biological Science Research Council (research grant no. 83/P09868 to P.P. and C.C.), and by the European Union-funded European *Gramineae* Mapping Project consortium (to F.Z.).

* Corresponding author; e-mail schlef@mpiz-koeln.mpg.de; fax 49–221–5062–313.

Article, publication date, and citation information can be found at www.plantphysiol.org/cgi/doi/10.1104/pp.010954.

mildew compatibility (Schultheiss et al., 2002). The exact biochemical mechanisms by which MLO proteins function have yet to be determined, and with the exception of barley MLO, none of the MLO proteins has been ascribed any biological function.

To widen the basis for structure/function analysis of the barley MLO protein, we describe previously unsequenced *mlo* resistance alleles, of which two confer partial *Bgh* resistance. We use the partial *mlo* resistance alleles and mutations in *Ror* genes to connect a previously unreported *Bgh*-triggered hydrogen peroxide (H_2O_2) burst at and cell death of mesophyll cells with the resistance response. The occurrence of spontaneous mesophyll cell death after leaves reach their final size, and the kinetics of leaf pigment removal in *mlo* plants suggest a role for wild-type *Mlo* in delaying leaf senescence. *Mlo* expression was found to be upregulated in response to pathogen inoculation and under a range of other stress conditions. These data imply that the wild-type *Mlo* gene plays a broad role in cell death protection, defense, and stress response processes.

RESULTS

mlo-16 and *mlo*-30 Are Defective in Intron Splicing

We added to the collection of characterized *mlo* resistance mutations (Büschges et al., 1997) by determining the DNA sequence of six additional *mlo* resistance alleles (designated *mlo*-12, -16, -27, -28, -29, and -30), each derived from chemical mutagenesis of susceptible *Mlo* wild-type plants (Habekuss and Hentrich, 1988; see "Materials and Methods"). All of the mutant alleles were found to contain single nucleotide substitutions in *Mlo*. Four of the mutations result in single amino acid changes, and they identify additional critical residues for MLO function in the second and third intracellular loop of the 7-TM protein (Table I). The two remaining mutations, present in *mlo*-16 and -30, are each located in intron sequences, and affect conserved nucleotides at intron-exon boundaries known to be critical for transcript splicing (Table I; Goodall and Filipowicz, 1991).

Reverse transcriptase (RT)-PCR from *mlo*-16 revealed one *Mlo* transcript with a 25-nucleotide deletion of exon 10 resulting from the use of a cryptic 3′-splice acceptor site in exon 10, and a transcript containing the entire unspliced intron 9 (Fig. 1A). Both of these mRNAs contain in-frame premature stop codons. RT-PCR from *mlo*-30 revealed one transcript containing an 18-nucleotide deletion of exon 12 sequences resulting from the use of a cryptic 3′-splice acceptor site in downstream exonic sequences, and another containing the entire unspliced intron 11 (Fig. 1B). These transcripts encode a protein with a six-amino acid in-frame deletion in the C-terminal cytoplasmic tail, and a severely truncated protein, respectively. RNA-blot analysis using an *Mlo* probe revealed additional transcripts in *mlo*-16 and -30, which were substantially smaller than the wild-type *Mlo* transcript, and which were not detected by RT-PCR (Fig. 1, A and B). In addition, correctly spliced transcripts were not detected for *mlo*-16 or for *mlo*-30 by RT-PCR. Thus, resistance of *mlo*-16 and -30 lines is due to severely reduced amounts of correctly spliced transcripts (encoding wild-type MLO) and/or compromised activity of abnormal MLO proteins resulting from incorrect splicing events.

Resistance Conferred by *mlo*-12 and *mlo*-28 Is Partial

Barley lines homozygous for the six newly sequenced *mlo* resistance alleles and 11 *mlo* resistance alleles sequenced by Büschges et al. (1997) were inoculated with fungal spores, and infection phenotypes were macroscopically and microscopically compared. Fifteen of the alleles (*mlo*-1, -3, -4, -5, -7, -8, -9, -10, -13, -16, -17, -26, 27, -29, and -30) allowed no fungal growth, whereas two of the newly sequenced alleles (*mlo*-12 and -28) allowed some sparse fungal hyphae growth. The size of the colonies on these partially resistant lines was smaller compared with wild-type *Mlo* plants at 7 d after fungal inoculation (Fig. 2). The complete and partial *mlo*-resistant lines, but not wild-type *Mlo* lines, showed host tissue necrosis at sites of attempted fungal invasion at 7 d after inoculation (Fig. 2). Frequencies of epidermal cell wall penetration by the fungus on the *mlo*-12 and -28 lines were determined to be between 18% and 35% (complete *mlo* resistance alleles = 0.8%; wild-type *Mlo* = 56%).

Table I. *Novel mlo alleles*

Nucleotide nos. based on the genomic *Mlo* DNA sequence starting from the translational start site (ATG).

Allele	Mutant IDs[a]	Mutational Event at *Mlo*	Effect on MLO Protein	Protein Domain Affected	*Bgh* Resistance	Mutagen
mlo-12	Do 4122	$C^{1396} \rightarrow A$	$F^{240} \rightarrow L$	Second intracellular loop	Partial	Nitrosomethylurea
mlo-16	Do 2376	$G^{1917} \rightarrow A$[b]	Not applicable	Not applicable	Full	Ethymethane sulfonate (EMS)
mlo-27	Do 2021[c]	$G^{2004} \rightarrow A$	$G^{318} \rightarrow E$	Third intracellular loop	Full	EMS
mlo-28	Do 4228	$C^{1224} \rightarrow T$	$T^{222} \rightarrow I$	Second intracellular loop	Partial	NaN_3
mlo-29	This study	$C^{2051} \rightarrow T$	$P^{334} \rightarrow L$	Third intracellular loop	Full	NaN_3
mlo-30	Do 2234, 2235	$A^{2242} \rightarrow T$[d]	Δ 6 amino acids	C terminus (intracellular)	Full	EMS

[a] According to Habekuss and Hentrich (1988). [b] Nucleotide substitution in the conserved 3′ splice site of intron 9. [c] Also Do 2002, 2003, 2004, 2005, 2014, 2015, 2016, and 2019. [d] Nucleotide substitution in the conserved 3′ splice site of intron 11.

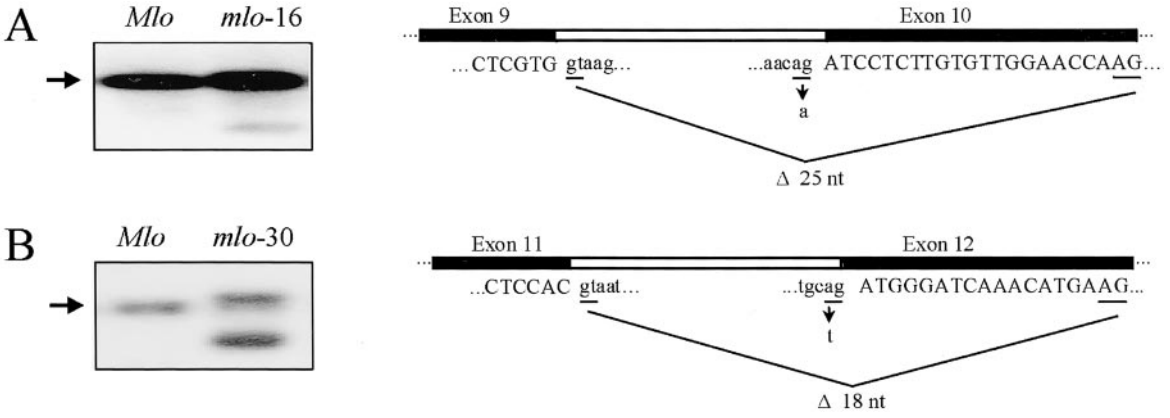

Figure 1. Characterization of two splicing-defective *mlo* mutant alleles. RNA-blot analysis (mRNA panels) and schematic representation of transcript splice products in *mlo*-16 (A) and *mlo*-30 genotypes (B). Northern-blot analysis was performed as described in "Materials and Methods" using wild-type *Mlo* plants as a control. Arrows indicate the *Mlo* wild-type transcript. Exonic sequences in the schematic representations are in uppercase and intron sequences in lowercase. Underlined dinucleotides in lowercase denotes 5′-splice donor and acceptor sites, and the underlined dinucleotides in uppercase represent the cryptic 3′-splice acceptor sites utilized in the *mlo*-16 and *mlo*-30 alleles. The arrows highlight the point mutations in *mlo*-16 (G→A) and *mlo*-30 (A→T) genotypes. Major splicing events in mutant cDNAs and corresponding effects on *Mlo* coding sequences are indicated by black lines.

Bgh-Triggered H_2O_2 Production and Mesophyll Cell Death Is Coupled with *mlo* Resistance

A cell wall-localized H_2O_2 burst occurs directly beneath sites of attempted epidermal cell penetration by *Bgh* in *mlo*-resistant and *Mlo*-susceptible barley lines (Freialdenhoven et al., 1996; Hückelhoven et al., 1999). This epidermal oxidative burst is greater in resistant *mlo* mutants than in susceptible (wild-type *Mlo*) plants and is modified by *Ror* genes (Hückelhoven et al., 2000). We quantified H_2O_2 accumulation 24 h after inoculation at sites of attempted epidermal cell wall penetration in near-isogenic genotypes containing wild-type or defective alleles of *Mlo* or *Ror1*, using computer image analysis of 3,3′-diaminobenzidine (DAB) polymerization (Fig. 3, A and B, and "Materials and Methods"). Measurements were taken at 24 h after inoculation, by which time the outcome of the penetration attempt has normally been determined. The susceptible *Mlo Ror1* genotype and the partially susceptible double mutant *mlo*-5 *ror1*-2 produced similar levels of H_2O_2, whereas the fully resistant *mlo*-5 *Ror1* genotype showed greater H_2O_2 levels (Fig. 3B), demonstrating a correlation between the production of cell wall-restricted H_2O_2 and resistance.

A second previously unreported oxidative burst occurs at mesophyll cells of *mlo* lines that subtend attacked epidermal cells (Fig. 3C, top). This H_2O_2 burst occurred approximately 36 h after spore inoculation, at least 16 h after the fungal penetration normally takes place. Approximately 60 h after spore inoculation, membranes of these mesophyll cells became irreversibly damaged as indicated by trypan blue retention (Fig. 3C, bottom). The mesophyll cell death response becomes macroscopically visible as localized necrosis 5 to 6 d after pathogen challenge (Fig. 2). DAB staining and trypan blue retention in the mesophyll were impaired in *mlo*-5 *ror1*-2 double mutants and were undetectable in wild-type *Mlo Ror1* plants (Fig. 3C), demonstrating

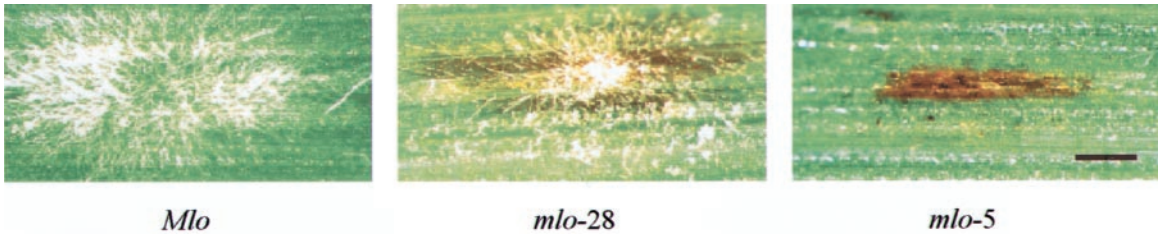

Figure 2. Bgh-triggered cell death in a partially resistant *mlo* mutant. Macroscopic phenotypes of wild-type *Mlo*, partially and fully resistant *mlo* mutants 7 d after fungal challenge. In the *Mlo* genotype (compatible interaction), no sign of cell death is visible beneath the sporulating colony. In the *mlo*-28 mutant (partially resistant), necrotic mesophyll cells are visible beneath a small fungal colony, and in the *mlo*-5 null mutant (fully resistant), a cluster of necrotic mesophyll cells can be seen beneath the failed penetration attempt. Bar = 50 μm.

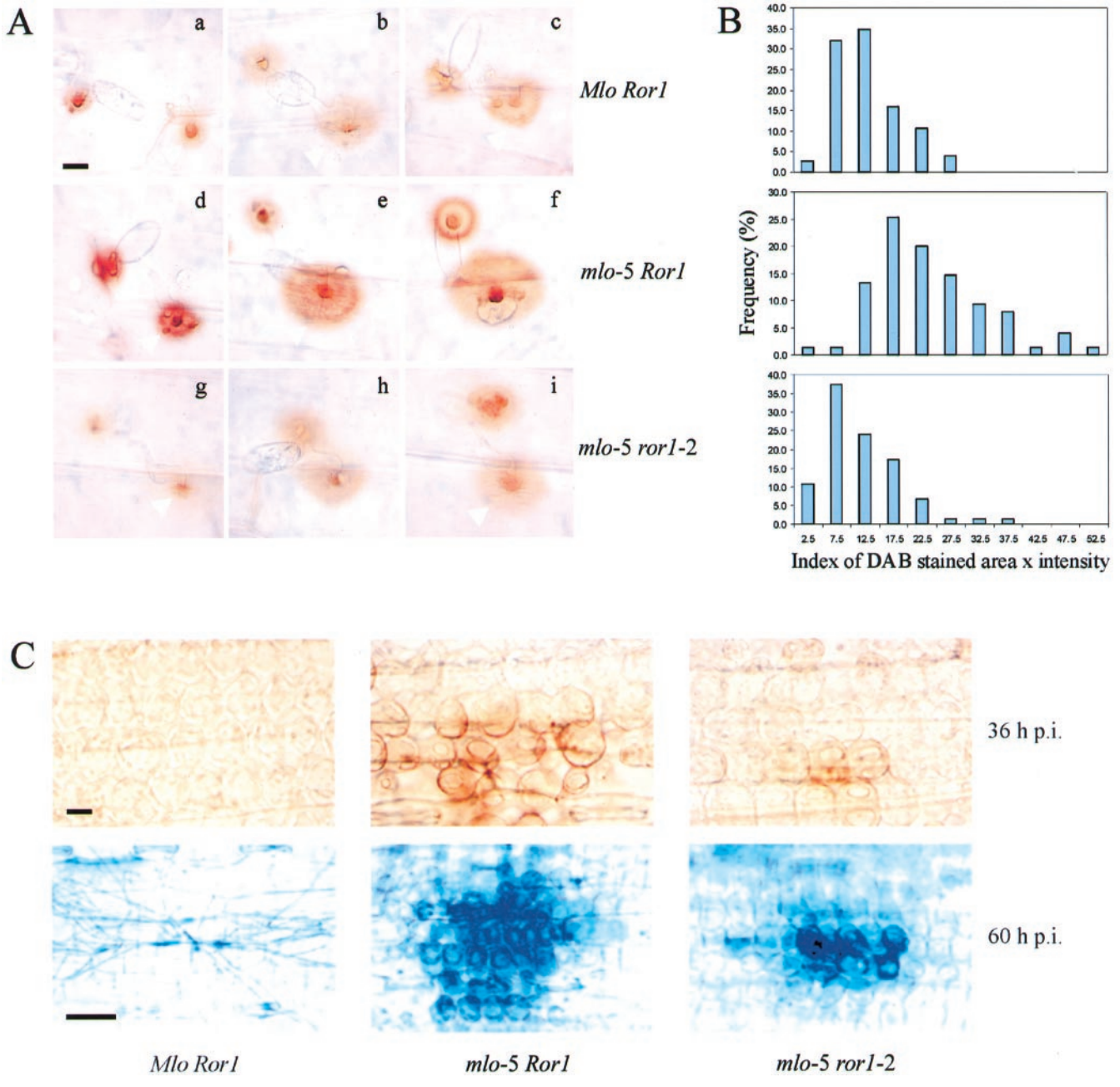

Figure 3. Inactivation of the MLO protein leads to enhanced H_2O_2 accumulation at epidermal cells and to cell death in the mesophyll. A, In situ detection of H_2O_2 by DAB precipitation at 24 h after inoculation. For each genotype, three sites are shown to illustrate the range of DAB staining (area and intensity) observed at sites of attempted fungal penetration (white arrow). Bar = 10 μm. B, Quantitative analysis of DAB-stained areas beneath fungal appressorial germ tubes (A, white arrows). C, DAB staining in mesophyll cells beneath sites of attempted penetration (top) at 36 h following inoculation; retention of trypan blue 60 h after fungal challenge (bottom). In the fully compatible interaction (*Mlo Ror1*), no DAB staining or trypan blue retention was observed. DAB staining and trypan blue retention were found to be significantly reduced in the double mutant *mlo*-5 *ror1*-2. Bar in top = 10 μm; bar in bottom = 50 μm.

that the mesophyll oxidative burst and the mesophyll cell death response are under control of *Mlo* and *Ror1*. The partially resistant mutants *mlo*-12 and -28 also exhibited the H_2O_2 and cell death response in the subtending mesophyll cells (data not shown), further demonstrating a link between resistance and the mesophyll H_2O_2 and cell death responses.

Premature Death of *mlo* Mutant Leaves Mimics Senescence

Axenically grown *mlo* mutants exhibit a spontaneous cell death phenotype, noticeable as premature leaf chlorosis (Wolter et al., 1993; Peterhänsel et al., 1997). We compared this premature death in *mlo*

plants with senescence of the first leaf normally observed in wild-type (*Mlo*) genotypes by monitoring markers for the latter. Leaf chlorophyll *a* and *b* and total carotenoid content increased indistinguishably in *Mlo* and *mlo*-5 genotypes during the first 17 d after sowing, after which the pigments began decreasing at a faster rate in *mlo*-5 than in *Mlo* plants (Fig. 4A). Carotenoids declined only marginally faster in the mutant leaves, consistent with their known relative stability during senescence (Biswal, 1995).

We monitored *Mlo*, ubiquitin, and glyceraldehyde-3-P dehydrogenase (GAPDH) mRNA levels by analyzing RNA samples from the same time course experiment. *Mlo* transcript abundance showed a gradual increase during the first 15 d after sowing (10- to 12-fold) in *Mlo* and *mlo*-5 leaves, which preceded the onset of the chlorophyll decline (Fig. 4B). Along with *Mlo* transcripts, ubiquitin transcripts increased markedly, but only in the *mlo*-5 line, possibly reflecting elevated protein degradation in the *mlo* leaves (for review, see Belknap and Garbarino, 1996). *GAPDH* transcripts declined in the *mlo*-5 mutant around 19 d after sowing, presumably reflecting a reduction in anabolic activity. The molecular changes observed in mutant and wild-type leaves preceded the first appearance of chlorosis, between 21 and 22 d after sowing in the *mlo*-5 line (Fig. 4C).

Mlo Expression Is Inducible by Biotic and Abiotic Stress

RNA-blot analysis showed that the *Mlo* mRNA in the leaf increased in abundance transiently after powdery mildew spore inoculation, indicating that *Mlo* expression is pathogen responsive (Fig. 5, A and B). This increase was observed in susceptible (*Mlo*) and resistant (*mlo*) genotypes, although the peak in abundance was more intense in the resistant genotype (14- versus 10-fold, respectively; Fig. 5, A and B). After returning to basal levels by 48 h, the *Mlo* transcripts increased again in abundance at 72 h, but only in the resistant genotype (Fig. 5, A and B). *Mlo* transcript changes followed an almost identical pattern to that of another pathogen-responsive gene encoding glutathione-*S*-transferase (GST; Fig. 5, A and B). A marked increase in *Mlo* transcript abundance

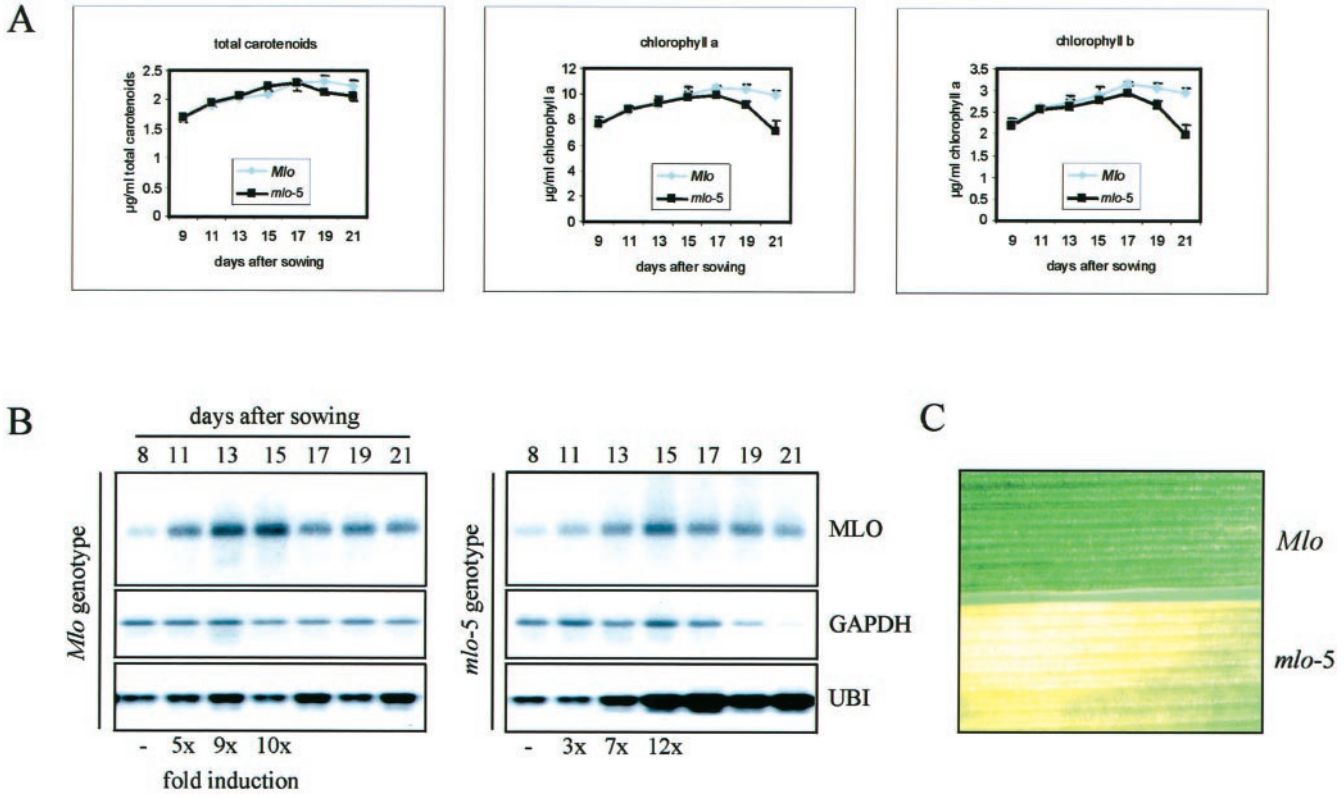

Figure 4. Accelerated leaf senescence in *mlo* mutants. A, Time course analysis of chlorophyll and carotenoid pigment content in *Mlo* wild-type and *mlo*-5 genotypes. First foliage leaves were collected at 2-d intervals from 9 to 21 d after sowing, and pigment analysis was carried out as described in "Materials and Methods." Each time point in the graphs shows the mean (±SD) of six leaf samples. B, Time course analysis of MLO transcript abundance throughout first foliage leaf development in *Mlo* wild-type and *mlo*-5 genotypes. The same blot was probed sequentially with the MLO-, GAPDH-, and ubiquitin (UBI)-labeled cDNAs. The fold changes in MLO transcript abundance were calculated using the GAPDH signal as a control. C, Mid-portions of first foliage leaves primary leaves of 24-d-old seedlings of the *Mlo* (top) and *mlo*-5 (bottom) genotypes. Chlorosis (yellowing) and, at later time points, necrotic lesions are noticeable in the *mlo*-5 genotype.

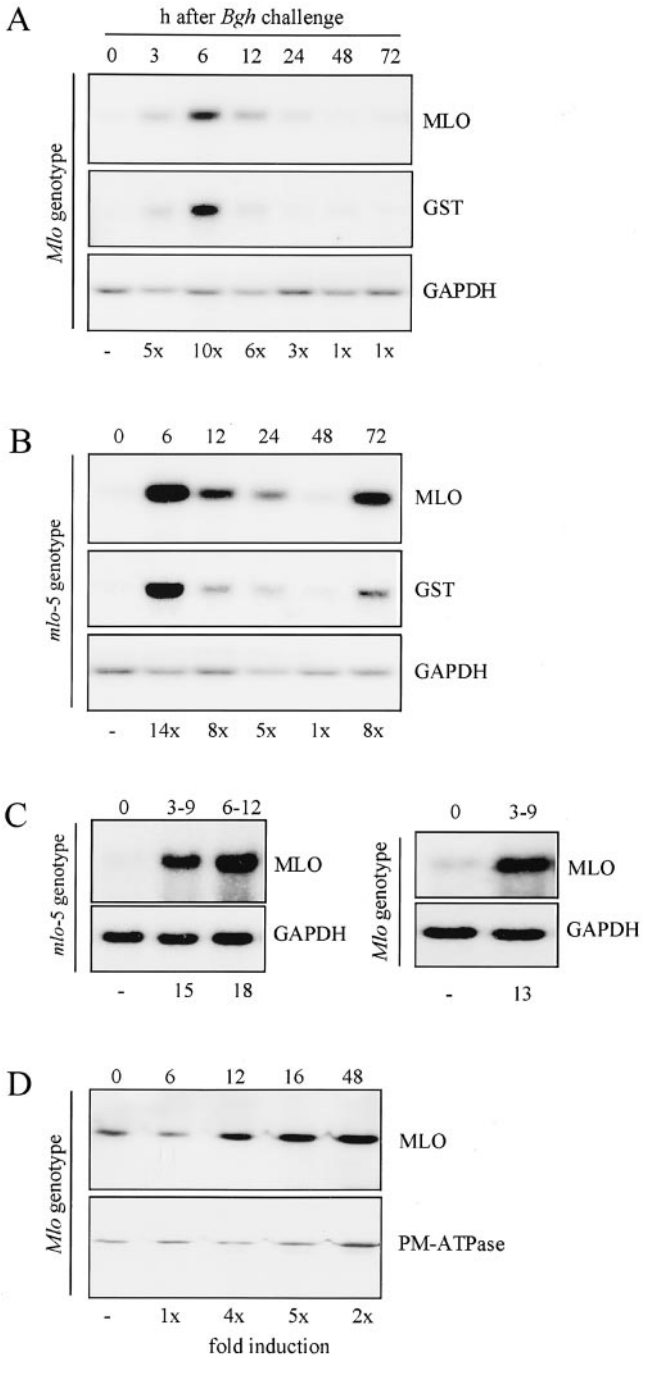

Figure 5. Time course analysis of MLO transcript and MLO protein upon powdery mildew inoculation. A and B, Accumulation of MLO transcript following *Bgh* challenge in *Mlo* wild-type (A) and *mlo*-5 (B) leaves. The same blot was sequentially probed with the MLO, GST, and GAPDH cDNA probes. The fold changes in MLO transcript abundance were calculated using the GAPDH signal as a control. The ×1 level was defined as ratio MLO:GAPDH ratio as at time 0. Figures showing MLO transcript levels were calculated using three independent experiments. C, Accumulation of MLO transcript following *Bgh* challenge in epidermal peels (see "Materials and Methods") of *mlo*-5 mutant (left) and *Mlo* wild-type (right) leaves. Abaxial leaf epidermal tissue was harvested during the indicated time intervals after spore inoculation, and the same blot was sequentially probed with the MLO and GAPDH cDNA probes. The fold changes in MLO transcript abundance were calculated using the GAPDH signal as a control. The ×1 level was defined as ratio MLO:GAPDH ratio as at time 0. D, Accumulation of MLO protein upon powdery mildew inoculation. Western blots of plasma membrane vesicle preparations from inoculated and uninoculated leaves were probed with the barley MLO-specific and the plasma membrane ATPase (PM-ATPase) antibodies. Positive signals were analyzed using a phosphor imager, and the fold MLO protein induction was calculated relative to the PM-ATPase signal. The ×1 level was defined as ratio MLO:PM-ATPase as at time 0. Figures showing MLO protein induction were calculated using two independent experiments.

was also detected in leaf epidermal peels of both genotypes, demonstrating pathogen-responsive gene expression in host cells that are in direct physical contact with the pathogen (Fig. 5C). Amounts of transcript accumulation were reflected by a 5-fold increase in MLO protein levels in enriched plasma membrane fractions, which peaked at 16 h after inoculation in the *Mlo* genotype (Fig. 5D; MLO-specific antibody described in Devoto et al., 1999). The time difference between transcript and protein accumulation peaks is consistent with the time required for polytopic membrane proteins to complete a series of maturation events, including endoplasmic reticulum insertion and trafficking via the Golgi to the plasma membrane (Hirschberg et al., 1998).

An increase in the amount of *Mlo* transcript was also observed after inoculation of barley with the rice (*Oryza sativa*) blast fungus *M. grisea*, indicating that *Mlo* expression is responsive to pathogens other than *Bgh* (Fig. 6A). However, unlike inoculation with *Bgh*, the second wave of transcript accumulation occurred in both genotypes instead of just the *mlo*-5 genotype. In the *mlo*-5 genotype, which is more susceptible to *M. grisea* (Jarosch et al., 1999), the second peak came approximately 72 h earlier than in the *Mlo* genotype, and continued increasing until at least 96 h after inoculation (Fig. 6A).

We tested additional treatments: a soluble carbohydrate elicitor derived from the wheat powdery mildew *B. graminis* f. sp. *tritici* (Schweizer et al., 2000), leaf wounding, and the herbicide paraquat. Each of these treatments up-regulated *Mlo* expression, but the peak of transcript abundance occurred at least 3 h earlier compared with that observed with the fungal inoculations (Fig. 6, B–D).

DISCUSSION

MLO Plays a Broad Role in Modulating Defense Responses and Cell Death

Host cell death is often associated with plant pathogen resistance, but may not always be required for the resistance per se (for review, see Shirasu and Schulze-Lefert, 2000). In the case of *mlo* resistance against *Bgh*, the mesophyll cells directly underlying the attacked epidermal cell respond with an H_2O_2 burst and then die (Fig. 3C). The mesophyll cell death

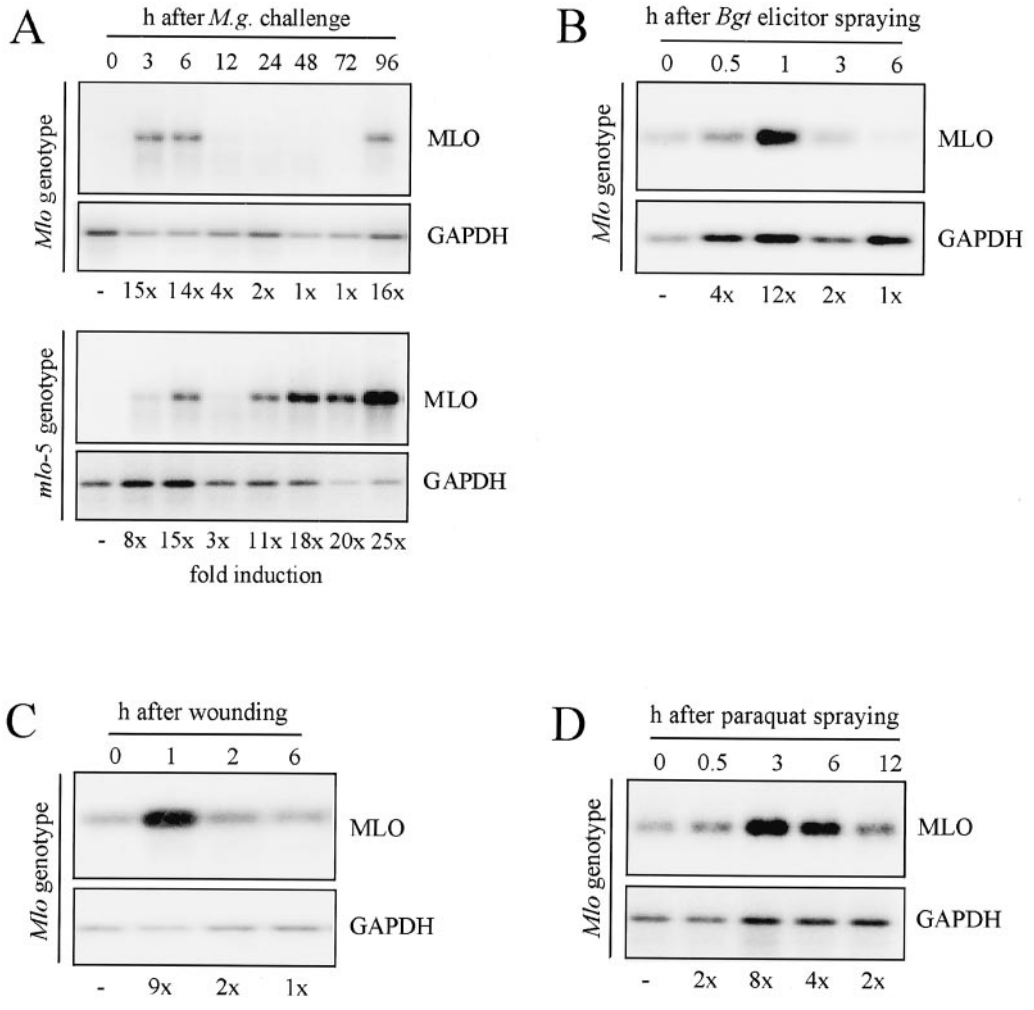

Figure 6. Time course analysis of MLO transcript accumulation upon *M. grisea* challenge and abiotic stresses. A, Accumulation of MLO transcript upon challenge of barley *Mlo* wild-type (top) and *mlo*-5 (bottom) leaves with *M. grisea*. The same blot was sequentially probed with the MLO and GAPDH probes. Signals were analyzed using a phosphorimager, and fold *Mlo* transcript accumulation was calculated using the GAPDH signal as control. Figures showing MLO transcript accumulation were calculated using two independent experiments. B, Accumulation of MLO mRNA upon a carbohydrate elicitor derived from the wheat (*Tritcum aestivum*) powdery mildew fungus (*Egt* elicitor). The same blot was probed sequentially with the barley MLO and GAPDH cDNAs. C, Accumulation of MLO mRNA upon wounding. First foliage barley leaves were harvested from 8-d-old seedlings and were mechanically wounded. Representative data from two independent experiments are shown. D, Accumulation of MLO mRNA upon paraquat treatment. Paraquat was sprayed onto 8-d-old seedlings to generate an oxidative burst in chloroplasts. After spraying, plants were kept for 2 h in the dark and were then transferred to light to ensure homogenous distribution of the chemical in the seedlings. The same blot was probed sequentially with the barley MLO and GAPDH cDNAs.

reaction is reduced in the partially susceptible *mlo*-5 *ror1*-2 genotype, is not observed in the wild-type *Mlo* genotype, and accompanies the *mlo*-12 and -28 partial resistance. The death of the mesophyll cells occurs after the fungal cell wall penetration attempt has halted (at about 60 versus 20 h) and the attacked epidermal cell remains alive, despite an earlier cell wall-localized H_2O_2 burst at the site of attempted penetration. Therefore, the *mlo* resistance is spatially and temporally separated from cell death, although the two processes are linked. *Mlo* is a suppressor of a defense reaction, such that loss of *Mlo* enhances the cell wall-restricted H_2O_2 burst (Fig. 3, A and B), the pathogen-induced expression of *PR* genes, and the size of fungal-induced papillae (Skou et al., 1984; Peterhänsel et al., 1997). Whether *mlo* plants exhibit mesophyll cell death because of the enhanced defense reaction (e.g. H_2O_2 production in the epidermis) or because the *mlo* mutation makes the mesophyll cells sensitive to cell death remains to be determined. It is not known whether the enhanced production of reactive oxygen species at sites of attempted fungal penetration in *mlo* mutants directly contributes to aborting fungal growth. In an alternate manner, the fungus may have a means of suppressing H_2O_2 production, which is less effective when the

fungal growth is terminated early. The observation that the fully susceptible *Mlo Ror1* genotype and the partially susceptible *mlo*-5 *ror1*-2 genotype produced similar levels of H_2O_2 in the epidermis (Fig. 3B) implies that factors other than reactive oxygen species must contribute to fungal abortion.

Perhaps unexpectedly, mutations in *Mlo* result in enhanced susceptibility to the rice blast fungus *M. grisea* (Jarosch et al., 1999), a hemibiotroph (Talbot and Foster, 2001), and the necrotrophic fungus *B. sorokiniana* (Kumar et al., 2001). It is an intriguing possibility that *mlo* mutations assist these pathogens in their necrotrophic lifestyles by triggering mesophyll cell death upon inoculation. In an alternate manner, wild-type *Mlo* may modulate different resistance mechanisms effective against biotrophic and necrotrophic fungi, in opposite directions.

In the absence of pathogens, first leaves of *mlo* plants become chlorotic and die several days earlier than those of *Mlo* plants (Fig. 4C). The premature leaf death resembled natural leaf senescence with regard to loss of pigments. Senescence of first (and second) foliage leaves in grasses (e.g. *Hordeum vulgare* and *Avena sativa*) has been well studied, and is a process that enables nutrients to be salvaged for incorporation into new growth. It begins soon after the leaves reach their final size (12–17 d after sowing), and involves a slow removal of chlorophyll and proteins (Miersch et al., 2000; Klerk and van Loon, 1997). Our data show that the onset of first foliage leaf senescence in *mlo* mutants remains unchanged while the speed is accelerated. Patches of mesophyll cell membrane damage appear in 18-d-old *mlo*-5 seedlings in a *Ror1*- and *Ror2*-dependent manner (Peterhänsel et al., 1997), coincident with the beginning of the leaf pigment decline reported in this study. It is possible that the accelerated senescence of *mlo* leaves is related to the mesophyll cell death clusters observed in leaves of an earlier age, as a cause or consequence of the latter. Irrespective of these interpretations, wild-type *Mlo* appears to play a broad role in delaying or preventing mesophyll cell death in pathogen-challenged and -nonchallenged leaves.

Control of *Mlo* Gene Expression

In wild-type *Mlo* plants, approximately 30% of fungal sporelings fail to penetrate the host epidermal cell wall as compared with 99.5% in *mlo* genotypes (Peterhänsel et al., 1997). Host reactions to *Bgh*, which are associated with *mlo* resistance such as vesicle congregation, papillae formation, a local cell wall-restricted H_2O_2 burst, and *PR* gene expression, are also observed in *Mlo* genotypes, albeit with less intensity (Peterhänsel et al., 1997). This suggests that wild-type *Mlo* is an incomplete suppressor of *mlo* resistance processes. Constitutive overexpression of wild-type *Mlo* in an *Mlo* background confers supersusceptibility to *Bgh* (Kim et al., 2002). Low constitutive levels of *Mlo* expression prior to *Bgh*-triggered induction of *Mlo* transcript accumulation may partly explain the incomplete resistance suppression by wild-type *Mlo*. At least part of the increase in *Mlo* expression appears to be taking place in the epidermis, which is the target tissue for *Bgh* (Fig. 5C). An increase in the plasma membrane MLO protein level becomes detectable by 12 h after inoculation (Fig. 5D), whereas penetration of the cell wall by *Bgh* occurs at about 15 h after inoculation (Peterhänsel et al., 1997). Therefore, the responsiveness of *Mlo* expression may be rapid enough to influence the level of *Bgh* compatibility in genotypes that encode an active MLO protein (*Mlo* genotype). Increased *Mlo* expression following pathogen attack may also be significant in protecting mesophyll cells from the H_2O_2 burst and mesophyll cell death responses otherwise seen in *mlo* genotypes from about 36 and 60 h after inoculation, respectively.

Before producing the appressorial germ tube, which contacts the leaf surface after about 10 h, *Bgh* spores produce a small primary germ tube that stops growing when it breaches the leaf surface after about 1 to 2 h (Carver et al., 1995). Therefore, the earliest observed increase in *Mlo* transcripts seen at 6 h after inoculation (Fig. 5, A and B) must occur before the attempted penetration, upon contact of the fungal spore or primary germ tube with the leaf.

H_2O_2, which is associated with and evokes defense and cell death processes in plants (Doke et al., 1996), is produced opposite to the *Bgh* primary and appressorial germ tubes (Thordal-Christensen et al., 1997). The more intense primary peak of *Mlo* induction in the *mlo* genotype corresponds with the more intense defense reaction in *mlo* plants, and the late induction peak observed in the *mlo* genotype only, at 72 h, corresponds with mesophyll H_2O_2 accumulation and cell death seen only in *mlo* plants. Elicitors and wounding are known to induce H_2O_2 production and other defense reactions (Doke et al., 1996; Lamb and Dixon, 1997), and the herbicide paraquat acts by triggering endogenous production of reactive oxygen species (Dodge, 1971). Induction of *Mlo* expression by these treatments is more rapid than that observed upon inoculation with *Bgh* or *M. grisea*, possibly reflecting the time needed for the pathogens to produce and transfer the microbial elicitor(s) to the host. Upon *M. grisea* inoculation, a second peak of *Mlo* induction occurs in *mlo*-5 and *Mlo* genotypes, although this begins about 72 h earlier in the *mlo*-5 genotype (Fig. 6A). In this case, *Mlo* induction is more conspicuously associated with the cell death that accompanies the interaction between the semi-necrotroph *M. grisea* and the susceptible *mlo* genotype than the enhanced *M. grisea* resistance of the *Mlo* genotype (Jarosch et al., 1999). *Mlo* is also induced in first leaves soon after the leaves reach their final size (10-d-old seedlings), and the maximum of transcript abundance coincides with the onset of detectable

molecular changes that are associated with senescence (Fig. 4). Thus, although the exact cues that lead to induction of *Mlo* expression are not yet known, these appear to be linked with cell death and/or defense processes.

It is curious that the induction of *Mlo* closely mirrors the expression of the cellular protectant *GST* (Fig. 5, A and B), suggesting that these two genes may be subject to similar control factors. Although the timing of this *Bgh*-induced transcript accumulation pattern appears to be different from those previously observed with defense-related genes, including *PR*-1, peroxidase, chitinase, and Phe ammonia lyase (Clark et al., 1994; Peterhänsel et al., 1997), they share a more intense accumulation in *mlo* compared with *Mlo* genotypes. The inducibility of *Mlo* expression under a range of conditions, plus the phenotypic consequences of *mlo* mutations, indicate a broad role for *Mlo*, which goes beyond modulation of *Bgh* resistance and associated cell death. This may have implications for elucidating the role(s) for the MLO protein family as a whole.

MATERIALS AND METHODS

Plant Material and Plant Treatments

Near-isogenic barley (*Hordeum vulgare*) lines cv Ingrid (susceptible wild type; *Mlo Ror1* genotype), back cross Ingrid *mlo*-5 (fully resistant null mutant; *mlo*-5 *Ror1* genotype; Büschges et al., 1997), and back cross Ingrid *mlo*-5 carrying the *ror1*-2 mutant allele (*mlo*-5 *ror1*-2 genotype; Freialdenhoven et al., 1996) were used for the experiments. Inoculation with *Bgh* spores was carried out as described by Freialdenhoven et al. (1996) using the powdery mildew isolate K1 (Hinze et al., 1991) on first leaves of 8-d-old seedlings grown under conditions described by Devoto et al. (1999). All experiments to investigate induction of *Mlo* transcript and MLO protein were performed at least three times. Epidermal peels of first leaves were obtained by making a transverse cut at the abaxial side and by removal of the epidermal layer using forceps. Inoculations with *Magnaporthe grisea* race 007 were carried out as described by Jarosch et al. (1999). Wheat (*Triticum aestivum*) powdery mildew elicitor kindly donated by Patrick Schweizer (IPK Gatersleben, Department of Cytogenetics, Germany; Schweizer et al., 2000) was sprayed on to 8-d-old barley seedlings at a concentration of 10 μg mL^{-1} Glc equivalents in 10 mM sodium phosphate buffer, pH 7.5, and 0.1% (w/v) Tween 20. Paraquat (methyl viologen; Sigma, St. Louis) was sprayed on to primary leaves of 8-d-old barley plants at a concentration of 50 μM in 10 mM sodium phosphate buffer, pH 7.5, and 0.1% (w/v) Tween 20, the plants were incubated in the dark for 2 h, and they were then transferred to light conditions (150 μmol photon m^{-2} s^{-1}). Wounding was carried out by making transverse cuts with a scalpel blade on primary leaves of 8-d-old seedlings, and the leaves were then floated on water.

Molecular Analysis of *mlo* Alleles

The additional *mlo* mutant alleles sequenced in this study were originally isolated by Habekuss and Hentrich (1988) except *mlo*-29, which was isolated by James Orme in this study following sodium azide mutagenesis of cv Sultan 5 *Mlo*. Genomic DNA sequences of *mlo* alleles were obtained by direct sequencing of PCR products. Using three sets of *Mlo*-specific primers, three overlapping fragments (each approximately 1.0 kb in size) were amplified using Expand HiFi *Taq* Polymerase (Roche Molecular Biochemicals, Summerville, NJ). PCR products were gel purified and subjected to direct sequencing.

DAB and Trypan Blue Histochemical Analysis

DAB uptake was carried out as described by Thordal-Christensen et al. (1997), fixing leaf samples at 24, 36, and 48 h after inoculation. DAB quantification was performed using the Scion Image analysis software (http://www.scioncorp.com/) to analyze 75 random penetration sites from six independent leaves per genotype. The program evaluates the color intensity of the stained area, quantifies its size, and calculates an index by multiplying the two values. Trypan blue retention was performed as previously described (Peterhänsel et al., 1997) using leaf segments collected 60 h postinoculation. Fungal penetration efficiencies were determined by examination of Coomassie Brilliant Blue R250-stained, lactophenol-treated, primary leaves of inoculated 8-d-old seedlings as described in Freialdenhoven et al. (1996). Occurrence of an intracellular haustorium in attacked epidermal cells was used as a measure for successful fungal penetration at single plant fungus interaction sites.

Northern-Blot, RT-PCR, and Western-Blot Analysis

Total RNA was isolated using the TriReagent (Sigma) protocol and poly(A)$^+$-enriched RNA fraction prepared using Oligotex columns (Qiagen, Valencia, CA). A final precipitation of the poly(A)$^+$ RNA was performed using glycogen (1/50 of original volume) and ethanol 100% (v/v; 2.5 volumes). Northern-blot analysis was carried out using standard procedures. Probes consisted of the full-length *Mlo* cDNA (Büschges et al., 1997; GenBank accession no. Z83834), the full-length cDNA encoding barley GAPDH (Chojecki, 1986; GenBank accession no. M36650), the *WIR5* wheat GST cDNA (Dudler et al., 1991; GenBank accession no. X56012), and the barley *mub1* ubiquitin cDNA (Gausing and Jensen, 1990; GenBank accession no. M60175).

First-strand cDNA was synthesized from 100 ng of poly(A)$^+$-enriched RNA using the oligo dT_{15} primer (Roche Molecular Biochemicals) and SuperScript RNase H$^-$ Reverse Transcriptase (Invitrogen, Carlsbad, CA). PCR was carried out using *Mlo* cDNA-specific primers and Expand HiFi *Taq* Polymerase (Roche Molecular Biochemicals). Western-blot analysis was performed as described previously (Devoto et al., 1999).

Chlorophyll and Carotenoid Quantification

Total chlorophyll *a*, chlorophyll *b*, and carotenoid levels were determined following the extraction procedure described by Wolfenden et al. (1988) with minor modifications. Three leaf discs (total fresh weight 0.25 g) were isolated from a primary leaf at 2-d intervals (expressed as days after sowing). Six leaves were analyzed at each time point. Data were analyzed and plotted using the Excel-5 program (Microsoft Co., Redmond, WA).

Received October 18, 2001; returned for revision February 19, 2002; accepted March 13, 2002.

LITERATURE CITED

Belknap WR, Garbarino JE (1996) The role of ubiquitin in plant senescence and stress responses. Trends Plant Sci **1:** 331–335

Biswal B (1995) Carotenoid catabolism during leaf senescence and its control by light. J Photochem Photobiol B Biol **30:** 3–13

Bockaert J, Pin JP (1999) Molecular tinkering of G protein-coupled receptors: an evolutionary success. EMBO J **18:** 1723–1729

Büschges R, Hollricher K, Panstruga R, Simons G, Wolter M, Frijters A, van Daelen R, van der Lee T, Diergaarde P, Groenendijk J et al. (1997) The barley *Mlo* gene: a novel control element of plant pathogen resistance. Cell **88:** 695–705

Carver T, Ingerson-Morris S, Thomas B, Zeyen R (1995) Early interactions during powdery mildew infection. Can J Bot Suppl 1 **73:** S632–S639

Chojecki J (1986) Identification and characterization of a cDNA clone for cytosolic glyceraldehyde-3-phosphate dehydrogenase in barley. Carlsberg Res Commun **51:** 203–210

Clark TA, Zeyen RJ, Smith AG, Carver TLW, Vance CP (1994) Phenylalanine ammonia lyase mRNA accumulation, enzyme activity and cytoplasmic responses in barley isolines, differing at *Ml-a* and *Ml-o* loci, attacked by *Erysiphe graminis* f.sp. *hordei*. Physiol Mol Plant Pathol **44:** 171–185

Devoto A, Piffanelli P, Nilsson I, Wallin E, Panstruga R, Heijne G, Schulze-Lefert P (1999) Topology, subcellular localization, and sequence diversity of the *Mlo* family in plants. J Biol Chem **274:** 34993–35004

Dietrich RA, Richberg MH, Schmidt R, Dean C, Dangl JL (1997) A novel zinc finger protein is encoded by the Arabidopsis *LSD1* gene and functions as a negative regulator of plant cell death. Cell **88:** 685–694

Dodge AD (1971) Mode of action of bipyridilium herbicides, paraquat and diquat. Endeavor **30:** 130–135

Doke N, Miura Y, Sanchez LM, Park HJ, Noritake T, Yoshioka H, Kawakita K (1996) The oxidative burst protects plants against pathogen attack: mechanism and role as an emergency signal for plant bio-defense: a review. Gene **179:** 45–51

Dudler R, Hertig C, Rebmann G, Bull J, Mauch F (1991) A pathogen-induced wheat gene encodes a protein homologous to glutathione-*S*-transferases. Mol Plant-Microbe Interact **4:** 14–18

Freialdenhoven A, Peterhänsel C, Kurth J, Kreuzaler F, Schulze-Lefert P (1996) Identification of genes required for the function of non-race-specific *mlo* resistance to powdery mildew in barley. Plant Cell **8:** 5–14

Frye CA, Innes RW (1998) An Arabidopsis mutant with enhanced resistance to powdery mildew. Plant Cell **10:** 947–956

Frye CA, Tang DZ, Innes RW (2001) Negative regulation of defense responses in plants by a conserved MAPKK kinase. Proc Natl Acad Sci USA **98:** 373–378

Gausing K, Jensen CB (1990) Two ubiquitin-long-tail fusion genes arranged as closely spaced direct repeats in barley. Gene **94:** 165–171

Goodall GJ, Filipowicz W (1991) Different effects of intron nucleotide composition and secondary structure on pre-mRNA splicing in monocot and dicot plants. EMBO J **10:** 2635–2644

Gray J, Close PS, Briggs SP, Joha GS (1997) A novel suppressor of cell death in plants by the *Lls1* gene of maize. Cell **89:** 25–31

Habekuss A, Hentrich W (1988) Charakterisierung funktionell verschiedener *mlo* Mutanten durch Primärinfektion, Pustelwachstum, Inkubationszeit und Befallsverlauf. Tag Ber Akad Landwirtsch-Wiss DDR, Berlin **272:** S-229–S-237

Hinze K, Thompson RD, Ritter E, Salamini F, Schulze-Lefert P (1991) Restriction fragment length polymorphism-mediated targeting of the mlo resistance locus in barley (*Hordeum vulgare*). Proc Natl Acad Sci USA **88:** 3691–3695

Hirschberg K, Miller CM, Ellenberg J, Presley JF, Siggia ED, Phair RD, Lippincott-Schwartz J (1998) Kinetic analysis of secretory protein traffic and characterization of Golgi to plasma membrane transport intermediates in living cells. J Cell Biol **143:** 1485–1503

Hückelhoven R, Fodor J, Preis C, Kogel KH (1999) Hypersensitive cell death and papilla formation in barley attacked by the powdery mildew fungus are associated with hydrogen peroxide but not with salicylic acid accumulation. Plant Physiol **119:** 1251–1260

Hückelhoven R, Trujillo M, Kogel KH (2000) Mutations in *Ror1* and *Ror2* genes cause modification of hydrogen peroxide accumulation in *mlo*-barley under attack from the powdery mildew fungus. Mol Plant Pathol **1:** 287–292

Jabs T, Dietrich RA, Dangl JL (1996) Initiation of runaway cell death in an Arabidopsis mutant by extracellular superoxide. Science **273:** 1853–1856

Jarosch B, Kogel KH, Schaffrath U (1999) The ambivalence of the barley *Mlo* locus: Mutations conferring resistance against powdery mildew (*Blumeria graminis* f. sp. *hordei*) enhance susceptibility to the rice blast fungus *Magnaporthe grisea*. Mol Plant-Microbe Interact **12:** 508–514

Jørgensen JH (1992) Discovery, characterization and exploitation of *Mlo* powdery mildew resistance in barley. Euphytica **63:** 141–152

Kim MC, Panstruga R, Elliott C, Müller J, Devoto A, Yoon HW, Park H, Cho MJ, Schulze-Lefert P (2002) Calmodulin interacts with MLO to regulate defense against mildew in barley. Nature **416:** 447–450

Klerk H, van Loon LC (1997) Characteristics of protein turnover in the developing first leaf of oats (*Avena sativa* L.). J Plant Physiol **151:** 176–187

Kumar J, Hückelhoven R, Beckhove U, Nagarajan S, Kogel KH (2001) A compromised *Mlo* pathway affects the response of barley to the necrotrophic fungus *Bipolaris sorokiniana* (Teleomorph: *Cochliobolus sativus*) and its toxins. Phytopathology **91:** 127–133

Lamb C, Dixon R (1997) The oxidative burst in plant disease resistance. Annu Rev Plant Physiol Plant Mol Biol **48:** 251–275

Miersch I, Heise J, Zelmer I, Humbeck K (2000) Differential degradation of the photosynthetic apparatus during leaf senescence in barley (*Hordeum vulgare* L.). Plant Biol **2:** 618–623

Peterhänsel C, Freialdenhoven A, Kurth J, Kolsch R, Schulze-Lefert P (1997) Interaction analyses of genes required for resistance responses to powdery mildew in barley reveal distinct pathways leading to leaf cell death. Plant Cell **9:** 1397–1409

Schultheiss H, Dechert C, Kogel KH, Hückelhoven R (2002) A small GTP-binding host protein is required for entry of powdery mildew fungus into epidermal cells of barley. Plant Physiol **128:** 1447–1454

Schweizer P, Kmecl A, Carpita N, Dudler R (2000) A soluble carbohydrate elicitor from *Blumeria graminis* f. sp. *tritici* is recognised by a broad range of cereals. Physiol Mol Plant Pathol **56:** 157–167

Shirasu K, Schulze-Lefert P (2000) Regulators of cell death in disease resistance. Plant Mol Biol **44:** 371–385

Simmons C, Hantke S, Grant S, Johal GS, Briggs SP (1998) The maize lethal leaf spot 1 mutant has elevated resistance to fungal infection at the leaf epidermis. Mol Plant-Microbe Interact **11:** 1110–1118

Skou J, Jørgensen J, Lilholt U (1984) Comparative studies on callose formation in powdery mildew compatible and incompatible barley. Phytopath Z **109:** 147–168

Talbot NJ, Foster AJ (2001) Genetics and genomics of the rice blast fungus *Magnaporthe grisea*: developing an experimental model for understanding fungal diseases of cereals. Adv Bot Res **34:** 263–287

Thordal-Christensen H, Zhang Z, Wei Y, Collinge DB (1997) Subcellular localization of H_2O_2 in plants: H_2O_2 accumulation in papillae and hypersensitive response during the barley-powdery mildew interaction. Plant J **11:** 1187–1194

von Röpenack E, Parr A, Schulze-Lefert P (1998) Structural analyses and dynamics of soluble and cell wall-bound phenolics in a broad spectrum resistance to the powdery mildew fungus in barley. J Biol Chem **273:** 9013–9022

Wolfenden J, Robinson DC, Cape JN, Paterson IS, Francis BJ, Mehlhorn H, Wellburn AR (1988) Use of carotenoid ratios, ethylene emissions and buffer capacities for the early diagnosis of forest decline. New Phytol **109:** 85–95

Wolter M, Hollricher K, Salamini F, Schulze-Lefert P (1993) The *mlo* resistance alleles to powdery mildew infection in barley trigger a developmentally controlled defense mimic phenotype. Mol Gen Genet **239:** 122–128